Phase Error Resilience to I/Q Mismatch of a Simplified CPM Receiver

Francisco A. Monteiro and António J. Rodrigues, *Member, IEEE*

***Abstract*—A low complexity receiver which was devised in previous papers proved there to be quasioptimum over additive gaussian noise and also showed low power penalty with flat Rayleigh fading, i.e., with random phase, and despite the fact that one of three reduced complexity blocks of that receiver relies on symmetries on signal's phase transitions. This letter analyzes the origin of that error resilience during the derivation of the metrics.**

***Index Terms*—Continuous phase modulation (CPM), phase rotation error, symmetry-based metrics derivation.**

I. Introduction

CONTINUOUS phase modulation (CPM) signals are insensitive to non-linear radio frequency (RF) amplitude amplification. Phase continuity allows good spectral performance and comprises a code gain. These properties motivated the widespread use of both MSK (minimum shift keying) and gaussian MSK. The use of other CPM schemes having both higher spectral and power efficiencies was restrained over time due to excessive detection complexity [1]. However, complexity reduction techniques made possible to employ CPM over digital radio relay links and it is also being considered for digital audio broadcasting [2].

CPM detection raises two problems: the optimum detector usually requires a very large bank of matched filters to obtain all phase transition metrics; afterwards, the number of phase states to track by a Viterbi algorithm may also be huge [1].

A quasi-optimum low complexity CPM receiver was achieved by introducing three complexity reduction techniques on the optimal receiver: *i)* replacement of the bank of matched filters by projections on a Walsh space [3]; *ii)* sequence detection with the M-algorithm [4]; and *iii)* a symmetry-based algorithm for the derivation of metrics from just 1/4 of them, which is to be further analyzed on this letter. This receiver has not only proved to be quasi-optimum when assessed only with additive gaussian noise (AWGN) [5] but also demonstrated just about 3 dB power loss when assessed over Rayleigh fading with both amplitude and phase additional impairments [6]. Hence, the geometric algorithm used to derive metrics proved robustness to phase rotations. This letter explains why and how that symmetry-dependent algorithm is resilient to phase rotations.

This work was supported in part by the Portuguese Foundation for Science and Technology under both POSI and FEDER programs.

F. Monteiro is with Instituto de Telecomunicações, Lisbon, Portugal, and with the Department of Information Science and Technology, ISCTE, Lisbon, Portugal (e-mail: frmo@lx.it.pt).

A. Rodrigues is with Instituto de Telecomunicações, Lisbon, Portugal, and with the Department of Electrical and Computer Engineering, Instituto Superior Técnico, Technical University of Lisbon, Portugal (e-mail: antonio.rodrigues@lx.it.pt).

II. CPM Signals and Testing Schemes

CPM signals are expressed by:

$$s(t,\boldsymbol{\gamma}) = \sqrt{2E_s/T_s}\,\cos(\omega_c t + \varphi(t,\boldsymbol{\gamma}) + \varphi_0)\,. \qquad (1)$$

The carrier frequency is f_c, where $\omega_c=2\pi f_c$, φ_0 is the arbitrary initial phase, and E_s is the energy per symbol, related with the bit energy by $E_s=\log_2(M)E_b$. Channel symbols are $\gamma_i\in\{\pm1, \pm3, \cdots, \pm(M\text{-}1)\}$, forming the M-ary sequence $\boldsymbol{\gamma}$. Each symbol γ_i carries $\log_2(M)$ bits as a result of a natural mapping of the information bits. The information carried by N_S channel symbols is keyed into signal's phase by

$$\varphi(t,\boldsymbol{\gamma}) = 2\pi h\sum_{i=0}^{N_s}\gamma_i q(t-iT_s)\,. \qquad (2)$$

A constant modulation index, $h=p/q$, is considered, where p and q are integers with no common factors, so that the number of phase states $S=2q$ is a finite one. Phase pulse shape, $q(t)$, affects phase transitions throughout L symbols, however, its effect remains until the end of the sequence. $q(t)$ is given by the frequency pulse $g(t)$: $q(t)=\int_{-\infty}^{t} g(\tau)d\tau$. Making $\int_0^{\infty} g(\tau)\,d\tau = 1/2$ assures that the maximum phase transition is $h\pi$ $(M-1)$ during a symbol time, T_s. The most common pulses are LREC and GMSK [1]. LREC is given by $g(t)=\text{rect}[t/(LT_s)]/2$, where $\text{rect}(t)=1$ for $-1/2<|t|<1/2$ and zero elsewhere.

The effect of phase rotations is initially studied for catastrophic M-ary CPM schemes ($h=1/2$, $M=2$, i.e. MSK, and for $M=4$, 8, and 16), taking advantage of their small number of states ($S=4$). Afterwards, the schemes 1REC $h=9/20$ with $M=4$ and 8 are tested. These schemes are the best 4 and 8-ary 1REC schemes in joint power and spectral efficiencies whilst preserving a low number of states ($S=40$). Moreover, both schemes have minimum normalized squared Euclidean distances (MNSED) equal to their upper bound [1, 3].

III. METRICS DERIVATION

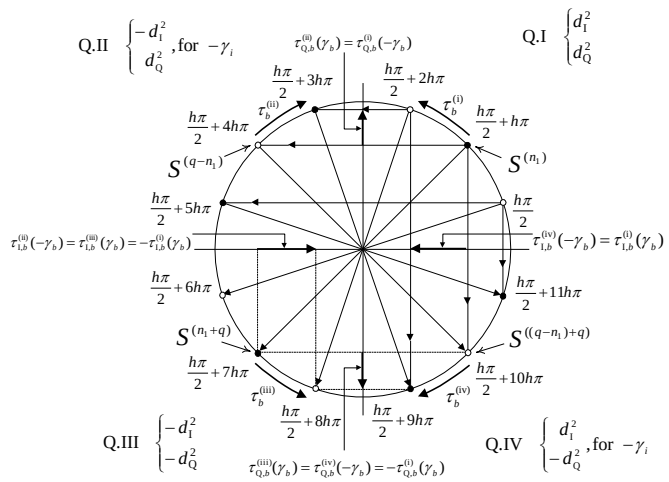

Fig. 1. Metric relations and coping procedures (example for h=1/6, S=12).

For schemes with S=0 mod 4 only transitions metrics of transitions departing from states on the first quadrant must be calculated, and only for the in-phase branch; all the others can be derived from them. The phase states of those schemes can be distributed throughout the four quadrants in a symmetric manner, placing $q/2$ states on each quadrant. Fig. 1 depicts a transition $\tau_b^{(i)}$ on the first quadrant and the relations of its both I and Q components with others on the remaining quadrants.

The principles underlying this derivation of metrics could be used to simplify the analog bank of matched filters, however with a baseband front-end like the one on [3] (just two integrators followed by sampling and simple algebra) that is needless. The derivation algorithm is of great convenience when used as the following block though. The technique is implemented using copy procedures among positions of a vector $\mathbf{\Lambda}_i$ (which holds the $\Xi=S\times M$ metrics for the i^{th} time interval) according to given rules. In detail, $\mathbf{\Lambda}_i$ stores each metric in a given fixed position. The positions are defined this way: the first position is reserved for the transition emerging from the first state (the one closer to 0ºon the first quadrant) and associated to the first possible channel symbol as ordered on the vector $\boldsymbol{\gamma}_\tau=[\gamma_\tau(1) = -(M-1),\ \gamma_\tau(2)=-(M-3),\cdots, -1, +1, \cdots, \gamma_\tau(M)=+(M-1)]$. The second position is reserved for the metric of the transition departing from the same state but defined by $\gamma_\tau(2)$. Therefore, the first M positions contain the metrics of all transitions emerging from the first state. Position M+1 is associated with the first transition from the second state. Thus, this periodic structure of M positions associated to each state allows to formulate an algorithm which maps the symmetries found on Fig. 1 into relations between positions of $\mathbf{\Lambda}_i$, as shown in Fig. 2 for a simple example with MSK.

For states number n_1=1, 2,···, S, on quadrants I, II, III, and IV, all metrics are obtained from a received symbol y_i doing:

1) Quadrant I: calculate the metrics for each M transition departing from each state inside the first quadrant and fill the

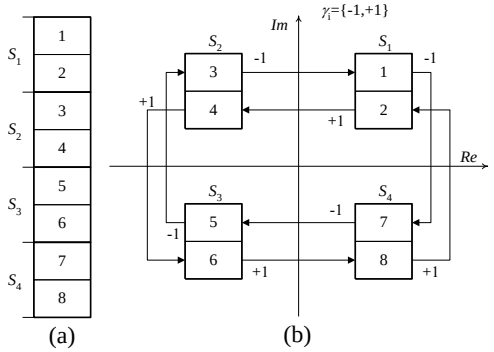

Fig. 2. Example for MSK. (a) Array with the Ξ=8 metrics. (b) Associations between array positions, phase states and phase transitions.

$\Xi/4$ positions of $\mathbf{\Lambda}_i$. Its first $\Xi/4$ positions will be referred by $b^{(\mathrm{I})} = n_1+n_2$ where states $S^{(n_1)}$ are associated to n_1=1, 2,···, $S/4$ and transitions emerging from it are linked to n_2=1, 2,···, M. Each metric is always the sum of the corresponding branch metrics, and for the first quadrant they are given by

$$\Lambda_{\mathrm{I}}(b^{(\mathrm{I})}) = \mathbf{y}_i \cdot \left(\boldsymbol{\tau}_{\mathrm{I}}(b^{(\mathrm{I})})\right)^{\mathrm{T}} \tag{3a}$$

$$\Lambda_{\mathrm{Q}}(b^{(\mathrm{I})}) = \mathbf{y}_i \cdot \left(\boldsymbol{\tau}_{\mathrm{Q}}(b^{(\mathrm{I})})\right)^{\mathrm{T}}. \tag{3b}$$

Using $\sin(\varphi)=\cos(\varphi - \pi/2)$ and considering mod Ξ operations, the Q metrics can also be obtained via

$$\Lambda_{\mathrm{Q}}(b^{(\mathrm{I})}) = \mathbf{y}_i \cdot \left[\boldsymbol{\tau}_{\mathrm{I}}\left(\left(b^{(\mathrm{I})} - \frac{q}{2}M\right) \bmod\left(\frac{\Xi}{4}\right)\right)\right]^{\mathrm{T}} \tag{4}$$

Metrics for quadrants II, III and IV are to be derived from those $\Xi/4$ metrics using the following relations:

2) Quadrant II: metrics of transitions initiating in states $S^{(q-n_1)}$ are copied from positions $b^{(\mathrm{I})}$ to positions $b^{(\mathrm{II})}$ for the symmetric symbol of $\boldsymbol{\gamma}_\tau$ (due to the inverse rotations plotted in Fig. 1) respecting $\Lambda_{\mathrm{I}}(b^{(\mathrm{II})}) = -\Lambda_{\mathrm{I}}(b^{(\mathrm{I})})$ and $\Lambda_{\mathrm{Q}}(b^{(\mathrm{II})}) = \Lambda_{\mathrm{Q}}(b^{(\mathrm{I})})$, for $b^{(\mathrm{II})}= (q+1-n_1)M+(M+1-n_2)$.

3) Quadrant III: For states $S^{((q-n_1)+q)}$, metrics should be copied from $b^{(\mathrm{I})}$ to positions $b^{(\mathrm{III})}$ following $\Lambda_{\mathrm{I}}(b^{(\mathrm{III})}) = -\Lambda_{\mathrm{I}}(b^{(\mathrm{I})})$ and $\Lambda_{\mathrm{Q}}(b^{(\mathrm{III})}) = -\Lambda_{\mathrm{Q}}(b^{(\mathrm{I})})$, for $b^{(\mathrm{III})} = b^{(\mathrm{I})}+q = n_1+n_2+qM$.

4) Quadrant IV: For the states $S^{((q-n_1)+q)}$, metrics should be copied from $b^{(\mathrm{I})}$ to positions $b^{(\mathrm{IV})}$ respecting $\Lambda_{\mathrm{I}}(b^{(\mathrm{IV})}) = \Lambda_{\mathrm{I}}(b^{(\mathrm{I})})$, and $\Lambda_{\mathrm{Q}}(b^{(\mathrm{IV})}) = -\Lambda_{\mathrm{Q}}(b^{(\mathrm{I})})$, for $b^{(\mathrm{IV})} = b^{(\mathrm{II})}+q = (q+1-n_1)M + (M+1-n_2)+qM$.

IV. METRICS DERIVATION UNDER PHASE ROTATIONS

The signal's reference phase φ_0 changes over time either owing to the channel or as a result of faulty receiver synchronism, both corresponding to a phase rotation, $\Delta\varphi$, on the complex signal space. Figs. 3 and 4 illustrate the effect on bit error rate (BER) of different fixed rotations for the schemes described in section II. Furthermore, the research revealed that for h=0.5 schemes one gets BER=0.5 at $\Delta\varphi$=45º and also at periodic multiples of this angle. The same

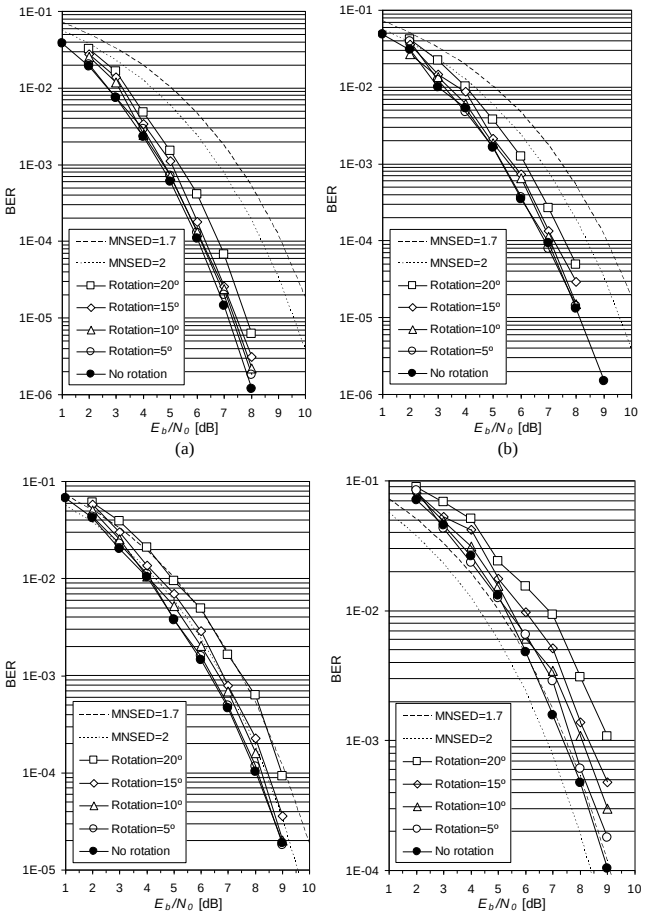

Fig. 3. Comparison of BER for 1REC, h=1/2. (a) M=16. (b) M=8. (c) M=4. (d) M=2.

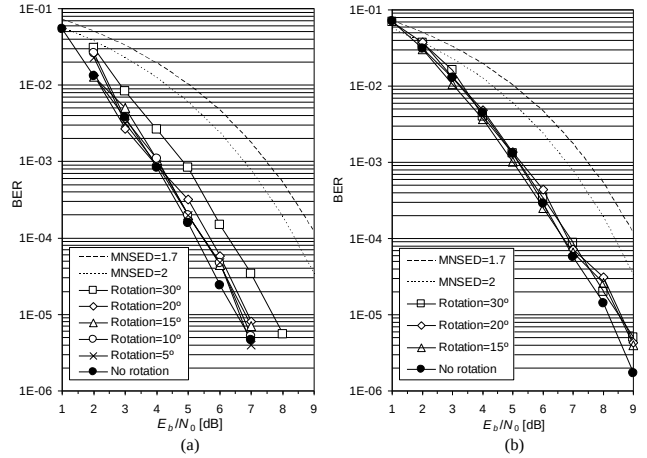

Fig. 4. Comparison of BER for 1REC, h=9/20. (a) M=8. (b) M=4.

maximum BER occurs for h=9/20 schemes at $\Delta\varphi$=40.5º plus at periodic multiples of that angle, revealing a periodic pattern in terms of power loss (measured for BER=10^{-4}) as a function of $\Delta\varphi$. Fig. 5 illustrates, with a simple example, the impact of nonzero $\Delta\varphi$ on in-phase transition components. It can be seen that projections of image-states appear on both I and Q branches. These consequences are further described by Fig. 6.

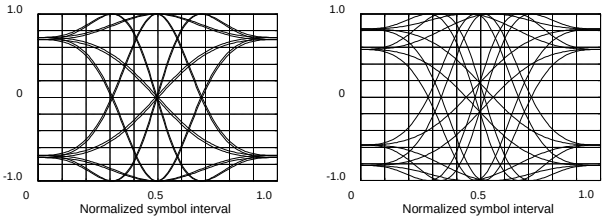

Fig. 5. In-phase transitions due to rotations for h=1/2, M=4. (a) 1º. (b) 10º.

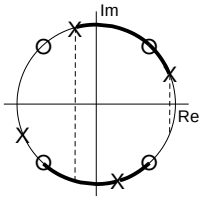

Fig. 6. Mismatch of original and derived transitions with phase rotation.

V. Conclusion

The correlation of the phase transition functions on each branch exhibits periodic values over $\Delta\varphi$. Initially, at $\Delta\varphi$=0, perfect symmetries exist (Fig.1). Despite symmetries are broken for incremental errors (Fig. 5(a)), some correlation remains (Fig. 5(b)). However orthogonality appears when $\Delta\varphi=\pm nh\pi/2$, for n integer, and therefore error peaks arise for rotations multiple of $h\pi/2$. One should notice that for h=1/2 this value is $\pi/4$ and that for h=9/20=0.45 the value becomes 40.5º, precisely the values found by simulation. The sequence detection block [4] is the only block dealing with signal's memory. Moreover, metric derivation is itself a memoryless process depending upon differential phase evolutions rather than absolute ones. In brief, the method adjusts itself to phase rotations and performance decays gradually over periodic phase error windows, which explains the resilience of the receiver with uniformly distributed random phase under fading [6]. Additionally, phase error compensation could be done with I/Q calibration [7], albeit not mandatory.

References

[1] J. Anderson, T. Aulin, and C. Sundberg, *Digital Phase Modulation*. New Yourk: Plennum Press, 1986.

[2] G. de Boer, C. Kupferschmidt, D. Bederov, and H.-P. Kuchenbecker, "Digital audio broadcasting in the FM band based on continuous phase modulation," *IEEE Trans. Broadcasting*, vol. 49, no. 3, pp. 293-303, Sep. 2003.

[3] F. Monteiro and A. Rodrigues, "Limits for CPM signals representation by Walsh functions," in *Proc. Eur. Conf. Wireless Technology*, Amsterdam, The Netherlands, Oct. 2004.

[4] ——, "The M-algorithm on the detection of CPM schemes on the minimum Euclidian distance upper bound," in *Proc. Eur. Conf. Wireless Technology*, Amsterdam, The Netherlands, Oct. 2004.

[5] ——, "CPM reception combining complexity reduction techniques for schemes on minimum Euclidian distance upper bound and MSK," in *Proc. IEEE Int. Symp. Information Theory*, Chicago, USA, Jun. 2004.

[6] ——, "Assessment of a quasi-optimum very low complexity CPM receiver over flat Rayleigh fading channels," in *Proc. IEEE Vehicular Technology Conf.*, Milan, Italy, May 2004.

[7] S. A. Chakra and B. Huyart, "Auto calibration with training sequences for wireless local loop at 26 GHz," *IEEE Microwave and Wireless Components Letters*, vol. 14, no. 8, pp. 392-394, Aug. 2004.